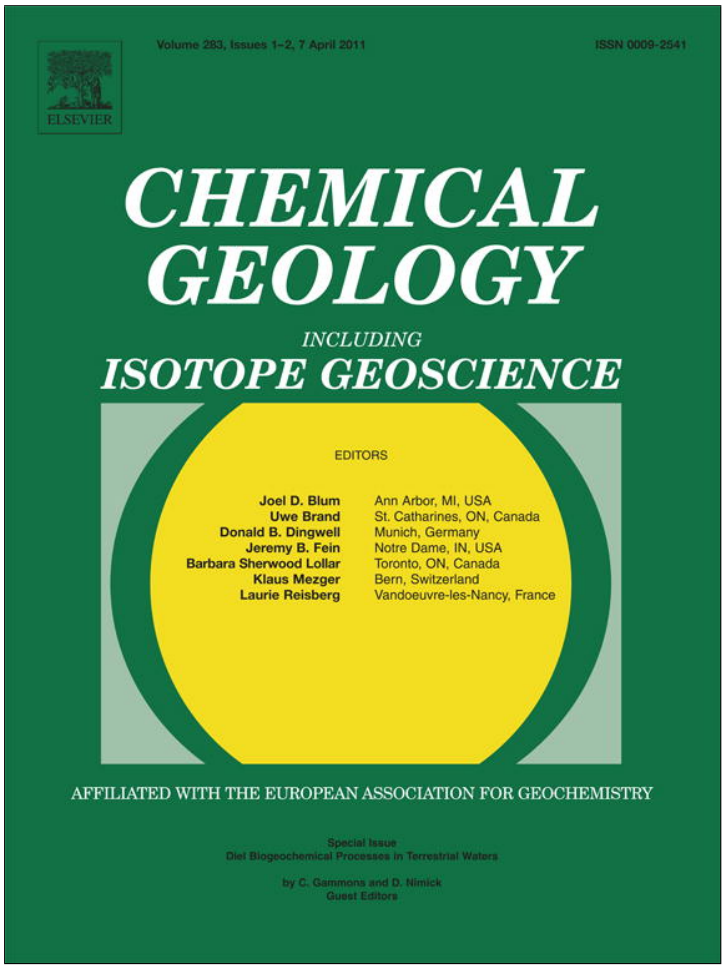

Chemical Geology 283 (2011) 87–98

Contents lists available at ScienceDirect

Chemical Geology

journal homepage: www.elsevier.com/locate/chemgeo

Trace element diel variations and particulate pulses in perimeter freshwater wetlands of Great Salt Lake, Utah

Gregory T. Carling, Diego P. Fernandez, Abigail Rudd, Eddy Pazmino, William P. Johnson *

Dept. of Geology & Geophysics, University of Utah, Salt Lake City, UT 84112, United States

ARTICLE INFO

Article history:
Received 15 May 2010
Received in revised form 20 October 2010
Accepted 3 January 2011
Available online 7 January 2011

Keywords:
Mercury
Antimony
Selenium
Uranium
Vanadium
Sorption

ABSTRACT

Trace elements (including total and methyl Hg, Sb, Se, U, V, and Mn), field parameters (including dissolved oxygen, pH, and water temperature), and other constituents were monitored over a 24-hr period during August 20–21, 2008 and September 14–15, 2009 at the outlet of two freshwater wetland ponds located near the southeastern shoreline of Great Salt Lake, Utah, to determine whether pe- and/or pH-driven diel cycles in trace element concentrations would be observed. Unfiltered and filtered (<0.45 μm) samples were collected hourly for all trace elements. Al, Fe, Hg, and Pb were predominantly (>75% of mass) associated with the >0.45 μm, or particulate, fraction. Cu, Cr, Cd, Mn, and Ti were also associated with the particulate fraction to a lesser extent (22–58% of mass). As, Co, Li, Ni, Sb, Se, Sr, U, and V were predominantly in the "dissolved" (<0.45 μm) form. Over a 24-hr period, the particle-associated elements displayed up to a factor of 5 differences between minimum and maximum concentrations, most likely due to settling and resuspension of particles in the water column. Of the dissolved trace elements, Sb, Se, U, and V concentrations showed a diel variation that was positively correlated with variations in dissolved oxygen, pH and water temperature: increasing following daybreak and decreasing at night. Concentrations of the dissolved fraction of Mn displayed the opposite trend relative to Sb, Se, U, and V. Diel trends in dissolved trace elements are explained by increased sorption of Sb, Se, U, and V anions during nighttime hours, and increased sorption of the Mn cations during daytime hours, driven by changes in water pH and temperature. Diel variations in the anion-forming elements Sb, Se, U, and V, although small in magnitude, support established trends of the anion-forming As. Methylmercury, which has been shown to vary on a diel cycle in other nearby locations, was consistently low at both ponds and displayed no diel trend.

1. Introduction

In studies characterizing trace element loads and toxicity in wetlands and streams, daytime measurements may not reflect variable concentrations that exist during a diel (24-hr) cycle due to photochemical processes and photosynthesis-driven changes in dissolved oxygen and pH. Mechanisms driving diel variations in trace elements include adsorption and desorption reactions, precipitation and dissolution, biological uptake, volatilization, sedimentation, and resuspension (Gammons et al., 2005, 2007; Jones et al., 2004; Krabbenhoft et al., 1998; McKnight and Bencala, 1988; Naftz et al., this issue; Nimick et al., 2003, 2005, 2007; Sullivan et al., 1998). Extensive work in alkaline streams has shown that divalent metal cations (e.g. Mn and Zn) tend to increase in concentration at night, while the anion-forming As tends to increase in concentration during the day (Barringer et al., 2008; Fuller and Davis, 1989; Gammons et al., 2007; Nimick et al., 1998, 2003, 2005). The opposing cycle in concentrations of divalent metal cations and anion-forming As has been attributed to pH- and temperature-induced sorption to stationary phases: cations are more effectively sorbed at higher temperature and pH (daytime conditions), while anions are more effectively sorbed at lower temperature and pH (nighttime conditions). While these cycles have been well examined for As, diel data for other anion-forming elements, such as Sb, Se, U, and V, are, to the authors' knowledge, absent in the literature.

Great Salt Lake (GSL), in the western United States, is a terminal lake which receives industrial, urban, mining, and agricultural discharge from a watershed with over 2 million people. The GSL ecosystem is vulnerable to contamination by a variety of harmful trace elements. For example, the concentrations of methylmercury (MeHg) measured in GSL are among the highest measured in surface water by the USGS Mercury Research Laboratory (Naftz et al., 2008). Also, applications for additional loads of selenium (Se) to GSL prompted development of a numerical standard for Se concentrations in the open water. An important aspect of developing numerical standards for Se and other trace elements is determining loads entering the lake from wetlands and streams, which typically rely on concentrations measured during daytime hours.

* Corresponding author.
E-mail address: william.johnson@utah.edu (W.P. Johnson).

0009-2541/$ – see front matter © 2011 Elsevier B.V. All rights reserved.
doi:10.1016/j.chemgeo.2011.01.001

The open water and adjacent freshwater wetlands of the GSL ecosystem support millions of migratory waterfowl and shorebirds from throughout the Western Hemisphere (Aldrich and Paul, 2002). For example, approximately half of all eared grebes (*Podiceps nigricollis*) spend the fall in GSL eating bring shrimp (*Artemia fransiscana*) to accumulate enough nutrients to fly to their wintering grounds in Mexico and California (Caudell and Conover, 2006). However, recent studies have reported elevated levels of Hg and Se in certain bird species which utilize GSL, including California gulls (*Larun californicus*), greenwinged teal (*Anas crecca*), and eared grebes (Conover and Vest, 2009a,b; Vest et al., 2009). In 2006 the Utah Department of Health issued consumption advisories for common goldeneye (*Bucephala clangula*), cinnamon teal (*Anas cyanoptera*), and northern shovelers (*Anas clypeata*) harvested from GSL marshes due to Hg concentrations which exceeded the USEPA guideline of 0.3 mg/kg (wet weight) in muscle tissue of these ducks (Scholl and Ball, 2006; USEPA, 2000).

The freshwater wetlands adjacent to GSL potentially act to decrease concentrations of trace elements in surface water prior to discharge to the lake via settling, adsorption, or mineral precipitation to sediment or aquatic vegetation (Dicataldo et al., 2011), volatilization (Diaz et al., 2009a), or biogeochemical transformations to less toxic species, such as reduction of Cr(VI) to less toxic Cr(III) (Mattuck and Nikolaidis, 1996). However, some biogeochemical transformations that occur in wetlands may actually produce more toxic species, such as the transformation of inorganic Hg to the highly toxic and bioaccumulative MeHg (e.g. Hall et al., 2008; Marvin-DiPasquale et al., 2003). MeHg is formed in oxygen-depleted water bodies or sediment with high nutrient and organic carbon loading that favor growth of sulfate and iron reducing bacteria (Benoit et al., 2003; Drott et al., 2007; Kerin et al., 2006; Lambertsson and Nilsson, 2006; Marvin-DiPasquale et al., 2009; Morel et al., 1998); conditions prevalent in wetlands receiving urban runoff (Chavan et al., 2007). Thus MeHg may be more effectively produced in wetlands during nighttime when suboxic or anoxic conditions prevail in the water column, as shown by Naftz et al. (this issue). Biogeochemical transformations may also lead to phase changes that alter trace element behavior. For example, particle-associated Hg may be more effectively methylated than dissolved Hg (Deonarine and Hsu-Kim, 2009), and particle-associated elements may be more effectively ingested by biota (Diaz et al., 2009b; Tarras-Wahlberg and Lane, 2003).

The purpose of this investigation is to characterize particulate and dissolved trace elements in the water column of an alkaline freshwater wetland adjacent to GSL to determine whether: 1) anion-forming trace elements other than As respond to the diel temperature, pH, and pe cycle; 2) concentrations of particle-associated trace elements vary over a diel cycle; 3) MeHg is produced during anoxic conditions which prevail in the wetland ponds during nighttime; and 4) the wetlands are net sources or sinks of trace and major elements.

2. Material and methods

2.1. Site description

Two freshwater wetland ponds at Ambassador Duck Club (ADC), located near the southeastern shoreline of GSL, were selected for diel surface water sampling (Fig. 1). The ponds have a surface area of approximately 0.25 km^2 and range in depth from 0.15 to 0.85 m. The ponds are hydrologically connected, with the upstream pond (i.e. Utah Storet Site 4985315 or ADC-1) draining towards the downstream pond (i.e. Utah Storet Site 4985320 or ADC-2) (Fig. 1). ADC-1 receives nutrient- and organic carbon-rich inflow from a canal which is derived in part from treated sewage effluent. Average inflow to ADC-1 is 3600 $m^3 h^{-1}$ and average water residence time in the ponds is approximately 30 h (Dicataldo et al., 2011). The ponds are an important habitat for a variety of ducks and other biota, including the common carp. Submerged aquatic vegetation (e.g. *Stuckenia* sp.) is common during late spring through fall, and duckweed (*Lemna* sp.) or algae mats occasionally cover the surface of the eutrophic ponds.

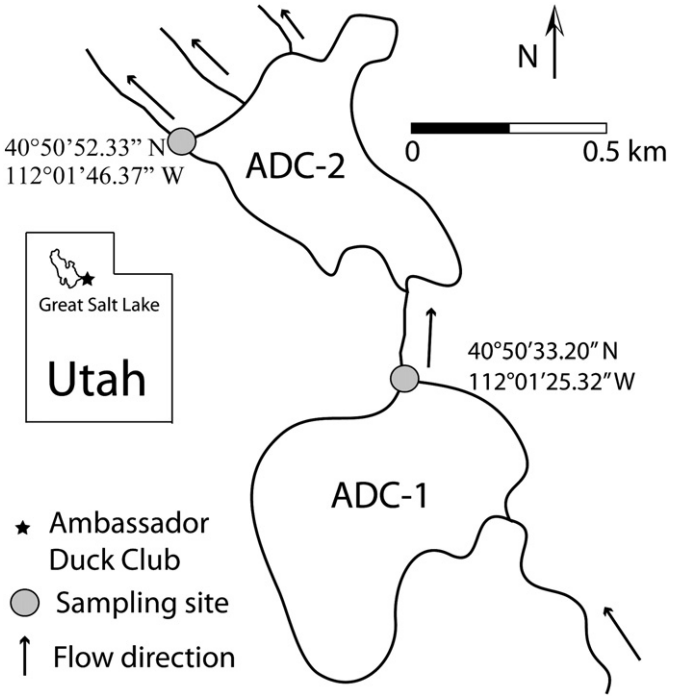

Fig. 1. Location of diel sampling sites (circles) at Ambassador Duck Club (ADC). Water samples were collected at the outlet of wetland ponds ADC-1 and ADC-2.

ADC-2 was the subject of earlier diel studies by Dicataldo et al. (2011). The previous work differs from the current investigation in that it focused on one pond with the objective of measuring diel concentrations of only a few trace elements (e.g. Se, As, and Mn). This paper has a broader scope with measurements made at both ADC-1 and ADC-2 of particulate and dissolved trace elements, including a wider range in analytes (e.g. total and methyl Hg, Sb, U, and V). This paper further substantiates limited Se and Mn data presented in Dicataldo et al. (2011).

2.2. Field methods

Unfiltered and filtered water samples for total Hg (THg), MeHg, trace elements and other constituents were collected hourly from mid-height in the water column at the outlet of ADC-1 and ADC-2 from 1300 h on August 20 to 1200 h on August 21, 2008, and from 1300 h on September 14 to 1200 h on September 15, 2009. Water at the pond outlet was assumed to integrate water chemistry of the entire pond. Unfiltered and filtered water samples for THg and MeHg were collected in serially rinsed FLPE bottles and acidified on-site to 1% v/v with trace metal grade HCl. Filtered and unfiltered water samples for other trace elements were collected in acid-leached LDPE bottles and acidified on-site to 2.4% v/v with trace metal grade HNO_3. THg, MeHg, and trace element samples were collected using strict "clean hands, dirty hands" protocols described in EPA Method 1669 (USEPA, 1996). During September 14–15, 2009, water samples for dissolved major ions and dissolved organic carbon were collected in amber HDPE bottles and amber glass containers, respectively. All water samples were stored in ice-filled coolers until the end of each sampling campaign and then transported to a fridge. Samples for major ions were stored frozen until analysis (USEPA, 1982). All equipment used for collecting, filtering, and processing water samples was acid-leached (i.e. 10% HCl for 2–3 days at 65 °C) or acid washed

(i.e. passing excessive volume of 10% HCl through apparatus) prior to field deployment. Field process blanks for all constituents were processed on site to determine potential contamination in the sampling process. New gloves and filtering equipment were used for each hourly sample set.

Water samples for THg, MeHg, and trace element analyses were filtered using two methods during August 20–21, 2008 to determine possible artifacts due to filter types: at ADC-1 water was collected in syringes (60 mL Excel International PE) and immediately forced through syringe filters (Whatman 0.45 μm PES), and at ADC-2 water was pumped through acid-washed Teflon tubing and forced through high-capacity capsule filters (Whatman Polycap GW 0.45 μm PES). In order to compare results of the two filtering methods, samples were collected for all constituents at both sites using both filtering methods. Results were similar (±10%) for THg and all other trace elements using both filtering methods. Likewise, similar concentrations (±10%) in the filtered fraction of all elements (besides Al, Cd, Fe, and Pb which were 20–40% higher at ADC-2) between the two ponds show that the filters produced equivalent results. Water samples for dissolved organic carbon (DOC) and filtered major ion analyses were not collected in 2008.

Water samples for trace element analyses were filtered using alternative methods during September 14–15, 2009. Aliquots of whole water samples were filtered (Whatman 0.45 μm PES) for trace element and major ion analyses at an indoor staging area within 15 min of sample collection. Aliquots of DOC samples were filtered within 24–48 h in the laboratory using a glass filtration apparatus and pre-fired glass fiber filters (Advantec Grade GF75). Water samples for filtered THg and filtered MeHg were not collected in 2009.

Field parameters were measured hourly at both sampling sites throughout both diel experiments. A Hydrolab Surveyor 4a multiparameter probe was used to measure dissolved oxygen (DO), water temperature (T_w), and specific conductance (SpC) at ADC-1. An In-Situ TROLL 9500 multiparameter probe was used to measure pH, DO, T_w, SpC, and stage (i.e. height of water column above a stationary reference point) at ADC-2. Instruments were calibrated using commercial standards for pH and SpC prior to each diel experiment. DO was calibrated using both an oxygen saturated and zero oxygen solution. Probe performance was cross-checked by taking the instrument from ADC-2 to ADC-1 to confirm that DO, T_w, and SpC were performing within 10% of one another. The instrument at ADC-1 was not fitted with a pH probe; thus potential drift was not checked. However, pH responded similarly to DO and T_w, indicating minimal drift in the measurement (Fig. 2). Semi-quantitative nitrite and sulfide concentrations were determined in the field on filtered (<0.45 μm) water samples within 15 min or less of sample collection with Chemetrics ampoules utilizing the colorimetric azo dye formation (USEPA method 354.1) and methylene blue (USEPA method 376.2) methods, respectively.

Sediment samples (top 10 cm; approximately 100 g wet sediment total) were collected from three locations at ADC-2 during the summer of 2010. Samples were capped in polyethylene tubes, sealed with electrical tape, and stored on ice.

2.3. Laboratory methods

THg and MeHg samples were analyzed within 3 months of collection using a Brooks Rand Model III CVAFS. THg and MeHg concentrations were determined according to EPA Method 1631e (USEPA, 2002) and 1630 (USEPA, 2001), respectively. At a minimum, matrix spike recoveries and replicates were analyzed for every 10 samples. For the sample run to be accepted, matrix spike recoveries had to fall within 75–125% of the original sample run and replicate analyses had to fall within ±10%. Method blanks were analyzed at the beginning of each run in order to calculate a daily detection limit (DDL). The accepted value for DDL is 0.4 ng/L and 0.02 ng/L for THg and MeHg, respectively, although lower detection limits are often achieved in our laboratory. Field process blanks were low for THg (n = 3, range 0.05–0.12 ng/L). In order to test accuracy of laboratory results, USGS standard reference samples (SRS) for THg were analyzed during each sample run, and results within ~10% of the accepted value were consistently obtained (supporting information, Table S1). Currently no SRS exist for MeHg. However, intercomparison tests on replicate MeHg water samples with the USGS Hg Research Laboratory in Middleton, Wisconsin show agreement between the two laboratories of ±20%.

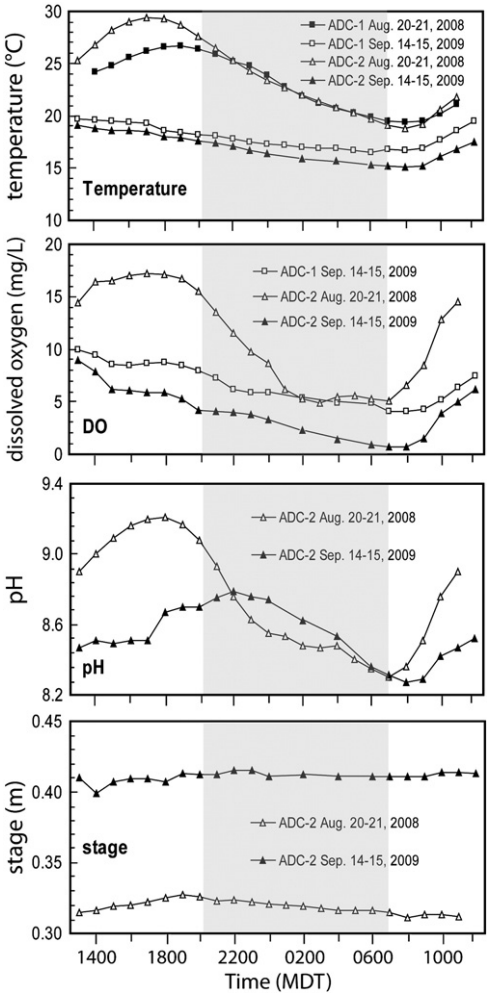

Fig. 2. Variation in water temperature, dissolved oxygen, pH, and stage at ADC-1 (squares) and ADC-2 (triangles) during August 20–21, 2008 and September 14–15, 2009. Shaded area indicates nighttime hours.

A quadrupole inductively coupled plasma mass spectrometer (ICP-MS) with a collision cell (Agilent 7500ce) was used to measure concentrations of Al, As, Ba, Cd, Co, Cr, Cu, Fe, Li, Mn, Ni, Pb, Sb, Se, Sr, Ti, U, V, and Zn on even hour samples. A quartz Scott-type cooled spray chamber with perfluoroalcoxy fluorocarbon (PFA) pumped nebulizer (0.4 mL/min) and a quartz torch was used. The sample, diluted 1:4 with 2.4% trace metal grade HNO_3 and internal standard (40 ng Tb/mL) were mixed in a Tee-union by means of a peristaltic pump using Tygon® tubing. Sensitivities of ~100 Mcps were obtained for solutions of 1 mg/L. A calibrating solution containing all the elements reported was prepared gravimetrically using 1000 mg/L single-element standards (Inorganic Ventures, Inc.). This solution was used to prepare a calibration curve with four points plus a blank. Cr, Fe, Mn, and V were determined using 4 mL He/min in the collision cell, while As and Se were determined using 2.5 mL H_2/min. Detection limit (DL) was determined as three times the standard deviation of

the 18 blanks analyzed throughout the run. A continuing calibration verification solution was prepared using SPEX LPC-1-100N multi-elemental standard containing Ag, Al, As, B, Ba, Be, Ca, Cd, Co, Cr, Cu, Fe, Li, Mg, Mn, Mo, Na, Ni, Pb, Sb, Se, Sn, Sr, Tl, V, and Zn (SPEX CertiPrep Group Inc.). This solution was diluted to 10 ng/mL and analyzed as a sample 6 times during each run. The agreement between measured and calculated values was better than 10% for all elements with the exception of Sb which had a measured value 50% larger than calculated. Also, USGS standard reference solutions T-193, T-195, and T-199 were run as samples to check the accuracy of the method. Agreements better than 10% between measured and average reported values were obtained for Cd, Cr, Cu, Pb and U, better than 20% for Co, Mn, Sr, and V, and between 25 and 35% for As, Fe, Li, and Ni (supporting information, Table S2). Field process blanks yielded values below or near detection limits for all elements with the exception of Ba and Zn; thus, data for Ba and Zn were not included in further analysis.

DOC samples were analyzed within one week of collection using a Shimadzu TOC-5000A. Fresh standards were created prior to analysis with potassium hydrogen phthalate for total carbon and sodium hydrogen carbonate and sodium carbonate for inorganic carbon.

Major anions (F^-, Cl^-, NO_3^-, and SO_4^{2-}) were analyzed using a Dionex 4100 ion chromatograph. Major cations (Na^+, K^+, Ca^{2+}, and Mg^{2+}) were analyzed using a Perkin Elmer 5100C atomic absorption spectrometer. Total alkalinity was measured using a Man-Tech QC Titrate with 0.02 N sulfuric acid. Standard procedures were followed for all major ion analyses, including the creation of calibration curves prior to each sample run, analysis of field and method blanks, and replicate analyses of at least 10% of samples. The average charge balance for all samples ($n = 26$) was −4.7%.

Sediment samples were homogenized in an Ar-filled glovebox by combining a small volume (e.g. 20 mL) of degassed Milli-Q water and mixing the slurry with an acid-washed plastic stirring utensil. Subsamples were taken for trace element analysis (1.0 g) and dry weight/total volatile solids (~25 g). Trace element extractions were performed by digesting sediment subsample in 20 mL 5% (v/v) trace metal grade HCl for three days at room temperature, followed by centrifugation and analysis of supernatant as a water sample (described above). Sediment dry weight and total volatile solids (TVS) were determined according to EPA Method 1684 (USEPA, 2001). Briefly, sediment was dried at 105 °C for 1 h, followed by ignition at 550 °C for 2 h (TVS was calculated as % loss on ignition).

2.4. Geochemical modeling

Aqueous speciation and saturation indices (SI) were calculated with PHREEQC using the Minteq.v4 thermodynamic database (Parkhurst and Appelo, 1999). Positive SI values, calculated as log (IAP/K_{sp}), indicate oversaturation and thermodynamic potential for mineral precipitation. PHREEQC uses ion-association and Debye Hückel expressions to account for the non-ideality of aqueous solutions. Distribution of elements among their valence states was estimated based on a specified range of pH and pe values. Averaged values from ADC-1 and ADC-2 of major ions, trace elements, and DOC were used in the simulations.

Surface-complexation reactions were modeled with PHREEQC using the generalized two-layer model of Dzombak and Morel (1990). Sb, Se, U, V, and Mn sorption on hydrous ferric oxide (Hfo) were simulated assuming the presence of weak sites on the oxide surface. In the simulations, ionic forms of Sb, Se, U, V, Mn, and other elements compete for binding sites, and equilibrium is described by mass-action equations. Activities of the surface species depend on the surface potential due to the development of surface charge. The simulations focused on sorption of Sb, Se, U, V, and Mn ionic species on Hfo as a function of field-measured pH and calculated pe values (based on the nitrite/nitrate redox couple). Properties of the Hfo surface were defined according to Dzombak and Morel (1990) with surface area of 600 $m^2 g^{-1}$ and solid mass concentration of 0.09 g. The number of sorption sites used was element-dependent, as described in Section 4.1.

3. Results

3.1. Pond water and sediment chemistry

T_w, DO, and pH varied on a diel basis with minima at dawn and maxima during afternoon hours (Fig. 2). T_w was measured at both sites during both field efforts; however, DO was not measured at ADC-1 during August, and pH was not measured at ADC-1 during August and September. We assume that DO and pH trends are correlated with T_w in ADC-1 as they are in ADC-2 (Fig. 2). The amplitude of the variation in T_w, DO, and pH was different among the two field efforts, likely due to seasonal influences as well as inter-annual variation in climate conditions. During August 20–21, 2008, T_w, DO, and pH ranged 19–30 °C, 5–15 mg/L, and 8.30–9.21, respectively; whereas, during September 14–15, 2009, the absolute values of these parameters were lower, ranging 15–19 °C, 0.8–10 mg/L, and 8.27–8.79 (Fig. 2). Nitrite concentrations were slightly elevated during nighttime hours (maximum of 0.15 mg/L) relative to daytime hours (minimum of <0.04 mg/L) during both diel sampling efforts. Sulfide concentrations remained at or below detection limit (0.2 mg/L) throughout the diel period, with no apparent increase during nighttime hours. Loss of sulfide during the period between sample collection and analysis (this holding time ranged between 3 and 15 min) was indicated negligible by consistent results regardless of holding time. Absence of significant sulfide was also indicated qualitatively by the lack of sulfide odor.

Major ions displayed no observable diel variations. Similar major ion concentrations were observed at ADC-1 and ADC-2 (salinities ~1000 mg/L). Some major ions were slightly higher in ADC-2 relative to ADC-1, i.e. Na^+ (170 mg/L versus 140 mg/L), Cl^- (260 mg/L versus 240 mg/L), HCO_3^- (255 mg/L versus 230 mg/L), and SO_4^{2-} (220 versus 205 mg/L). However, NO_3^- was significantly higher in ADC-1 relative to ADC-2 (23 mg/L versus 7 mg/L). Other major ions (Mg^{2+}, Ca^{2+}, K^+, and F^-) showed similar concentrations in ADC-1 and ADC-2. DOC concentrations averaged 13 mg/L in ADC-1 and ADC-2.

Sediment samples ($n = 3$) showed that trace element concentrations (reported here as dry weight) were elevated in sediment relative to surface water (Figs. 3, 4, and 5; SI-Figs. 2 and 3) for Al (4.2 ± 0.2 g/kg), Fe (4.0 ± 0.5 g/kg), Mn (353 ± 18 mg/kg), Sb (15.9 ± 1.5 μg/kg), Se (110 ± 20 μg/kg), Ti (60.0 ± 7.0 mg/kg), U (2.3 ± 0.3 mg/kg), and V (12.5 ± 1.0 mg/kg). Total volatile solids comprised 8.9 ± 0.8% of sediment mass.

3.2. Particulate and dissolved trace elements

The fraction of trace element mass associated with >0.45 μm suspended solids was calculated as the difference between unfiltered and filtered concentrations of each element. Based on averaged data collected at ADC-1 and ADC-2 during August 20–21, 2008 and September 14–15, 2009, three groups of trace elements were distinguished: 1) predominant particle-associated elements, with >75% of mass in the >0.45 μm fraction (Fe, Al, Hg, and Pb); 2) moderate particle-associated elements, with 22–58% of mass in the >0.45 μm fraction (Cu, Cr, Cd, Mn, and Ti); and 3) dissolved elements, which had similar concentrations (±7%) in both unfiltered and filtered samples (As, Co, Li, Ni, Sb, Se, Sr, U, and V) (supporting information, Table S3). Although the mass of a trace element that passes through a 0.45 μm filter is not necessarily dissolved, as the trace element may be associated with colloidal phases <0.45 μm, we hereby use the term "dissolved" for simplicity of discussion.

3.3. Diel variations in dissolved trace elements

Among the dissolved trace elements, some showed temporal variations (Fig. 3), albeit of lower magnitude than the particle-associated elements (described below; Fig. 5). Sb, Se, U, and V generally followed a diel cycle of increasing concentrations following daybreak and decreasing concentrations at night, with somewhat stronger diel variations at ADC-2 (Fig. 3B) relative to ADC-1 (Fig. 3A). The diel changes for some elements were small (results below), with amplitudes sometimes within analytical error. While general accuracy of the data is considered to be 10% (described in Section 2.3), in some of the datasets a clear diel trend is observed with an amplitude of ~10%, demonstrating that errors <10% were achieved under some circumstances (e.g. U in Fig. 3).

The diel cycles also showed seasonal/inter-annual differences, with U showing constant values at ADC-1 during August 20–21, 2008, but 10% variation (calculated as relative percent difference) during September 14–15, 2009 (Fig. 3A). Likewise, at ADC-1 during August 20–21, 2008, V concentrations varied by 14%, Se concentrations varied by 13%, and Sb concentrations varied by 10%; whereas, during September 14–15, 2009, V and Se concentrations remained relatively constant (Fig. 3A). Sb data is not shown for September 14–15, 2009 because it was below the detection limit (due to the relatively high detection limit of 2.5 μg Sb/L on the ICP-MS during these sample runs).

At ADC-2 during both diel sampling efforts, U concentrations varied by 7–11%, V concentrations varied by 19–36%, and Se concentrations varied by 20–26% (Fig. 3B). Sb concentrations varied by 13% during August 20–21, 2008 (Fig. 3B).

The dissolved (<0.45 μm) fraction of Mn followed an opposite trend relative to Sb, Se, U, and V, with decreasing concentrations following daybreak and increasing concentrations during nighttime hours (Fig. 4). At ADC-1 and ADC-2, filtered Mn concentrations varied 35–58% during the two diel sampling efforts (Fig. 4), with similar concentrations among the two ponds (in the range of 6 to 18 μg/L).

Notably, contrasting diel trends for Se and Mn, as described above, were also observed by Dicataldo et al. (2011) at ADC-2 during a diel study conducted Aug. 17–18, 2007. These authors also observed diel variations in As concentrations similar to Mn during a May 24–25, 2006 diel sampling. However our results showed no diel trend for As (supporting information, Fig. S1), or other dissolved elements Co, Li, Ni, and Sr.

3.4. Particulate trace element pulses

The unfiltered concentrations of particle-associated trace elements varied strongly over time (i.e. up to factor of 5 differences between daily minimum and maximum); whereas, relatively constant concentrations were observed for the filtered fraction (Fig. 5), with the

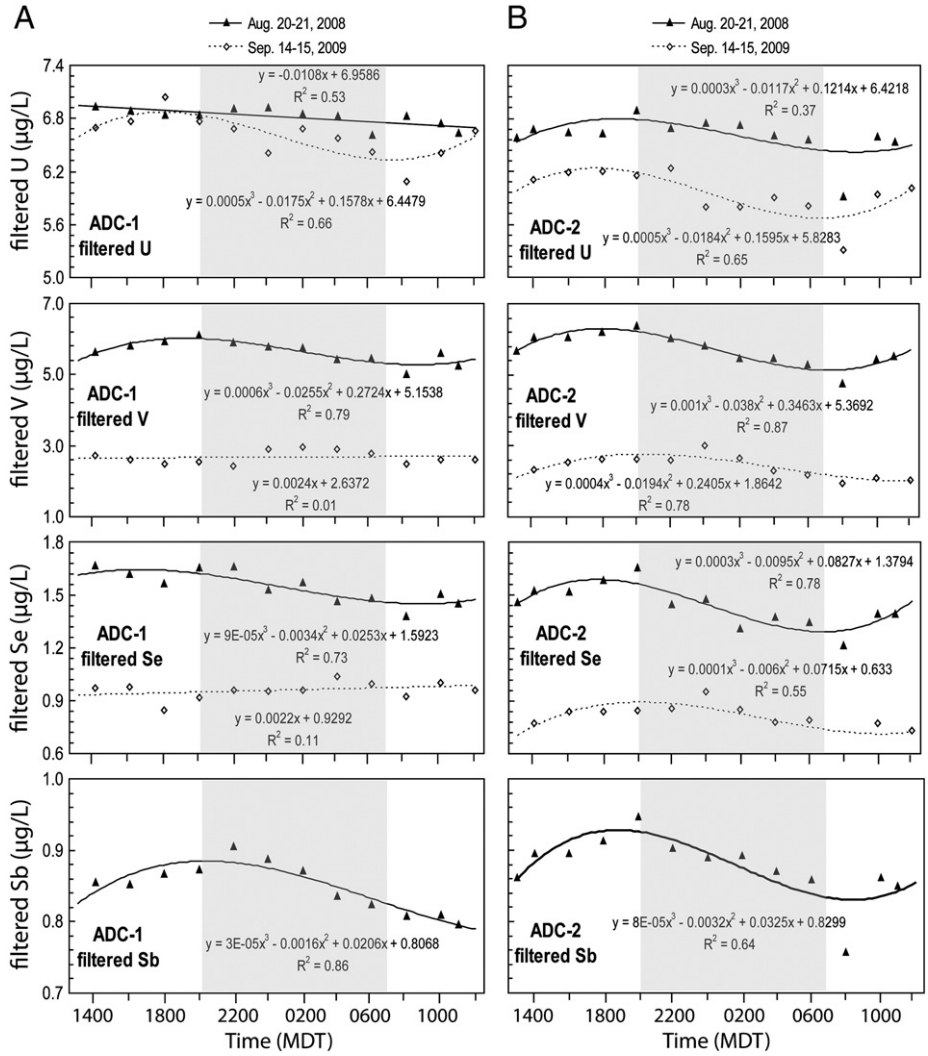

Fig. 3. Variation in dissolved trace element concentrations measured at (A) ADC-1 and (B) ADC-2 during August 20–21, 2008 (solid lines) and September 14–15, 2009 (dashed lines). Shaded area indicates nighttime hours. Data trends were fitted with a third order polynomial when warranted by a substantial increase in R^2 relative to a linear trend line.

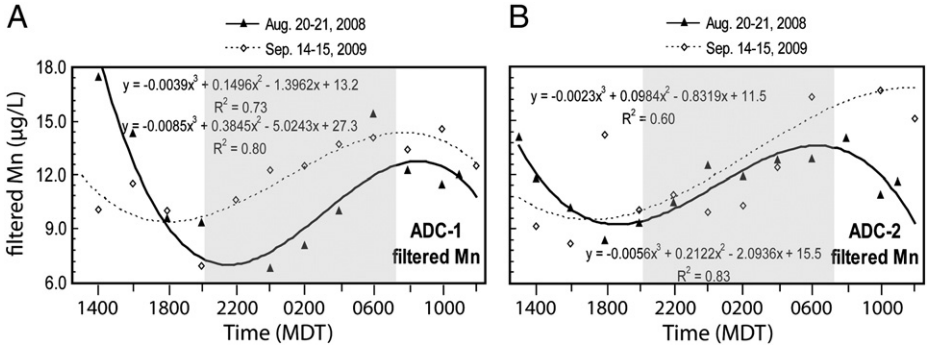

Fig. 4. Variation in filtered Mn concentrations at (A) ADC-1 and (B) ADC-2 during August 20–21, 2008 (solid line) and September 14–15, 2009 (dashed line). Shaded area indicates nighttime hours. Data trends were fitted with a third order polynomial as warranted by a substantial increase in R^2 relative to a linear trend line.

exception of filtered Mn (Fig. 4; as discussed above). The predominant particle-associated elements (Al, Fe, Pb, and Hg) showed larger variations than the moderate particle-associated elements (Cd, Cu, Cr, Mn, and Ti). At ADC-1, the predominant particle-associated elements showed factor of 3–5 differences between maximum and minimum concentrations during August 20–21, 2008 (Fig. 5A), and factor of 2 differences during September 14–15, 2009 (Fig. 5B). At ADC-2, the predominant particle-associated elements showed factor of 2–4 differences between maximum and minimum concentrations during August 20–21, 2008 (Fig. 5C), but during September 14–15, 2009 particulate concentrations were low and no significant changes in concentration occurred (Fig. 5D). Peak concentrations appear to be randomly distributed with time (although the peaks generally occur during the afternoon or nighttime hours), but the concentrations of different elements tend to peak at the same time. The moderate particle-associated elements showed similar trends as the predominant particle-associated elements, but with smaller magnitude of variation (i.e. maximum factor of 2 differences between maximum and minimum values; supporting information, Figs. S2 and S3).

3.5. Methylmercury concentrations

MeHg concentrations showed no diel variation in ADC-1 or ADC-2 during August 20–21, 2008, and were at or below DDL in ADC-1 and ADC-2 during September 14–15, 2009 (Fig. 6). MeHg concentrations were higher in ADC-1 than ADC-2 during both diel experiments (Fig. 6). MeHg concentrations during August 20–21, 2008 were a factor of 5 higher than concentrations during September 14–15, 2009 at both ADC-1 and ADC-2 (Fig. 6), but even the highest concentrations (0.2 ng/L) are near background levels found in uncontaminated sites (Gray and Hines, 2009).

4. Discussion

4.1. Origin of observed diel cycles of dissolved elements

To our knowledge, diel variations in concentrations of the anion-forming elements Sb, U, and V have not been previously reported in the literature, and diel trends for Se have only been reported for one diel cycle (Dicataldo et al., 2011). Diel variations in concentrations of the divalent metal cation Mn are well substantiated (e.g. Nimick et al., 2003, 2005). Notably, our results showed no diel trend for anion-forming As (supporting information, Fig. S1). A number of previous studies have documented diel variations of As in rivers and streams, with As concentrations reaching a maximum during daytime and a minimum during nighttime/early morning (Barringer et al., 2008; Fuller and Davis, 1989; Gammons et al., 2007; Nimick et al., 1998, 2003, 2005). The lack of observation of an As diel cycle in our study may have resulted from inhibition of sorption due to, e.g. As complexation with DOC. It is also possible that the lack of observation of a diel cycle for As was artifactual, due to interference of $^{40}Ar^{35}Cl$ on ^{75}As during ICP-MS analyses. Although kinetic discrimination apparently succeeded in eliminating the $^{40}Ar^{38}Ar$ interference on ^{78}Se, it is possible that this strategy was not successful for ^{75}As. Cl concentrations were significant (~250 mg/L), and ^{35}Cl comprises 75% of Cl isotopes.

Photosynthesis-driven changes in pH and DO controlled redox conditions in the surface water of the wetland ponds. The decrease in DO during nighttime hours (Fig. 2) and corresponding increase in nitrite, without production of sulfide, suggests that pond water geochemistry evolved towards nitrate-reducing conditions during nighttime hours, but did not evolve to anoxic conditions necessary for sulfate reduction. Of course the measurement at the pond outlet integrates varied geochemical conditions that may exist among pond environments (e.g. benthic versus littoral).

Diel trends for concentrations of aqueous Sb, Se, U, and V (Fig. 3) were positively correlated with T_w, pH and DO (Fig. 2), whereas filtered Mn concentrations followed an opposite trend (Fig. 4). This relationship suggests a pH- or redox- (i.e. pe) driven mechanism for observed diel variations of these elements (e.g. Nimick et al., 2003). Values of pe are difficult to measure or estimate; however, PHREEQC simulations using the nitrite/nitrate redox couple indicate a maximum pe value of 7 during the day when nitrite concentrations were at or near the detection limit (represented with <0.001 mg/L based on a 0.04 mg/L detection limit for nitrite), and a minimum pe value of 4 during the night with nitrite concentrations up to 0.15 mg/L. Dicataldo et al. (2011) justified a similar pe range on the basis of ORP measured during a diel cycle at the same wetland pond.

Over this pH and pe range, possible mechanisms for transferring Sb, Se, U, V, and Mn to and from the aqueous phase include either precipitation or sorption to stationary phases (e.g. sediment or submerged aquatic vegetation). PHREEQC simulations showed that across the pH range of 8.2–9.2 and the covarying pe range of 4–7 (estimated using the nitrite/nitrate couple, as described above), all mineral phases containing Sb, Se, U, or V had negative SI values, indicating that these elements were thermodynamically not likely to form mineral precipitates. However, at pH ≥ 8.9 a number of mineral phases containing Mn (e.g. bixbyite, hausmannite, pyrolusite, and manganite) showed positive SI values, indicating that Mn precipitation may occur with increasing pH and/or increasing oxidation potential. Thus, a possible explanation for the observed daytime decrease of Mn concentrations in the water column is precipitation of aqueous Mn to form minerals on stationary phases (e.g. sediment or submerged aquatic vegetation) as pH/pe increased during the day.

PHREEQC simulations showed that the anionic forms of Sb, Se, U, and V, and the cationic form of Mn were the most prevalent aqueous species under the observed pH/pe conditions. Sb was found almost entirely as the oxyanion SbO_3^- (i.e. +V oxidation state) across the

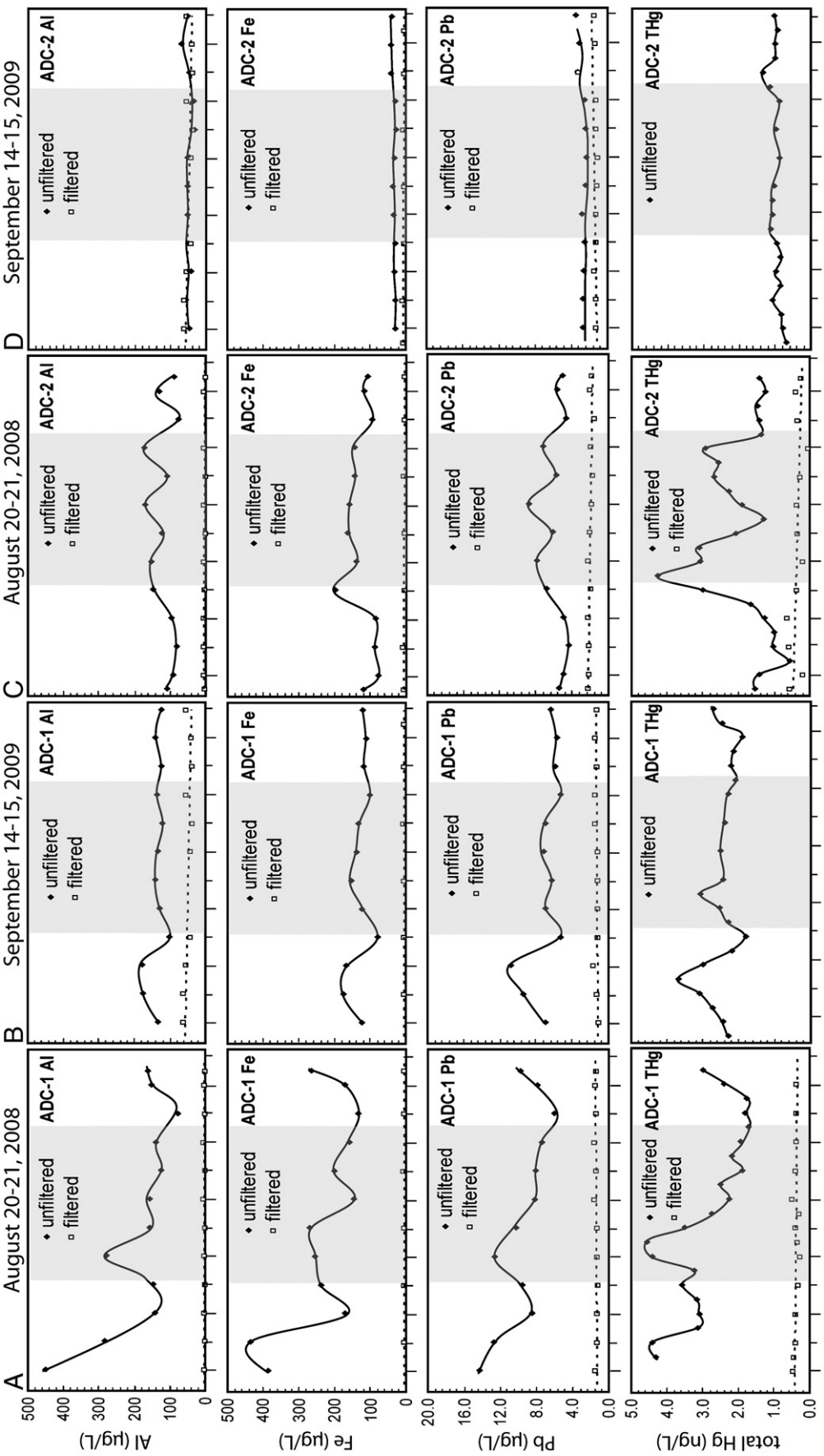

Fig. 5. Variation in predominant particulate trace element concentrations measured at ADC-1 (A, B) and ADC-2 (C, D) during August 20–21, 2008 (A, C) and September 14–15, 2009 (B, D). Solid line represents unfiltered concentrations and dashed line represents filtered concentrations; lines were hand-drawn. Shaded area indicates nighttime hours.

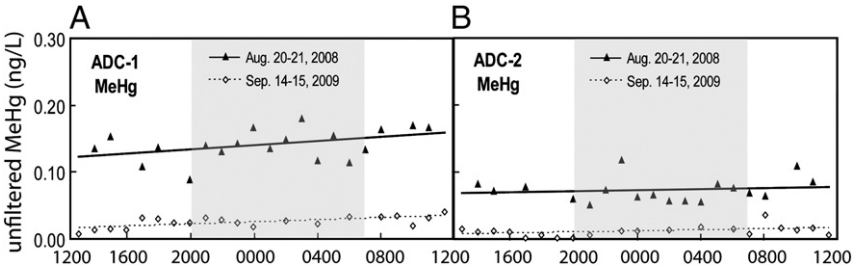

Fig. 6. Unfiltered methylmercury concentrations at (A) ADC-1 and (B) ADC-2 during August 20–21, 2008 (solid line) and September 14–15, 2009 (dashed line). Shaded area indicates nighttime hours. Data below DDL are shown for comparison purposes only.

observed range of pH and pe values; however, the literature shows that the hydrolytic form $Sb(OH)_6^-$ should be the dominant species (Filella and May, 2003; Martinez-Llado et al., 2008). Therefore, the SbO_3^- species was removed from the Minteq.v4 database for further simulations. U and V aqueous speciation were found to be sensitive to changes in pH but not pe. At pH ≤8.5, the uranyl dicarbonate anion $UO_2(CO_3)_2^{2-}$ (+VI oxidation state) was the predominant U species, and at pH ≥8.9, the uranyl tricarbonate species $UO_2(CO_3)_3^{4-}$ (+VI oxidation state) was predominant. At pH ≤8.5, the oxyanions $H_2VO_4^-$ (+V oxidation state) and HVO_4^{2-} (+V oxidation state) were found in similar proportions, but at pH >8.5, HVO_4^{2-} was the predominant species. Se was the only element sensitive to both pH and pe. At pH ≤8.5 and pe ≤5, Se existed predominantly as the selenite species SeO_3^{2-} and $HSeO_3^-$ (+IV oxidation state), and at pH ≥8.9 and pe ≥6, Se existed almost entirely as the selenate species SeO_4^{2-} (+VI oxidation state). Aqueous Mn was predicted predominantly as the cation Mn^{2+} across the observed pH/pe range.

In agreement with reports by Nimick et al. (2003, 2005) regarding As, anionic species (Sb, Se, U, and V) showed similar diel behavior of increasing concentrations during the day and decreasing concentrations at night (Fig. 3), whereas divalent metal cationic species (Mn) followed a reverse trend (Fig. 4). This indicates that the diel pH cycle may be driving anion sorption to a stationary phase (e.g. sediment or submerged aquatic vegetation) during the night, and cation sorption during daytime. Therefore, to test the plausibility of sorption as a mechanism for observed diel changes in the aqueous phase of these elements, an equilibrium surface phase (Hfo) was simulated in PHREEQC. Hfo was used to conceptually represent the presence of metal oxides, organic matter, and other phases that potentially undergo pH-dependent surface complexation with the anionic and cationic species. A substantial fraction of the bottom sediment at ADC-2 was composed of Fe (0.4 ± 0.05% dry weight, n = 3). Other metals were also present in the sediment (see Section 3.1), and organic matter comprised a considerable fraction of sediment mass (TVS 8.9 ± 0.8% dry weight, n = 3). We herein use Hfo as an easily-implemented example of the pH-dependence of trace element sorption to provide an explanation of the observed diel variations.

Weak binding sites on Hfo were considered using a nominal number of binding sites of 4×10^{-4} mol for simulating sorption of Sb, Se, and Mn. However, for U and V simulations, the number of binding sites was adjusted to 2.75×10^{-6} and 4×10^{-7} mol, respectively. Adjusting the number of binding sites is justified on the basis that Hfo sorption equilibrium expressions for U and V (described below) were adapted from experimental data using goethite, which is expected to display a higher site density relative to Hfo.

Equilibrium expressions for sorption of Sb, Se, U, V, and Mn on Hfo (below) were obtained from various sources. Eq. (1) was adapted from Martinez-Llado et al. (2008), Eqs. (2)–(5) were used directly from the Minteqv.4 database (Dzombak and Morel, 1990), Eqs. (6) and (7) were adapted from Mahoney et al. (2009) and Jung et al. (1999), respectively, Eqs. (8) and (9) were adapted from Peacock and Sherman (2004), and Eq. (10) was used directly from the Phreeqc database (Dzombak and Morel, 1990):

$$2Hfo\_wOH + Sb(OH)_6^- = Hfo\_w_2O_2Sb(OH)_4^- + 2H_2O \quad \log K_{eq} = 5.2 \tag{1}$$

$$Hfo\_wOH + HSeO_3^- = Hfo\_wSeO_3^- + H_2O \quad \log K_{eq} = 4.29 \tag{2}$$

$$Hfo\_wOH + HSeO_3^- = Hfo\_wOHSeO_3^{2-} + H^+ \quad \log K_{eq} = -3.23 \tag{3}$$

$$Hfo\_wOH + SeO_4^{2-} + H^+ = Hfo\_wSeO_4^- + H_2O \quad \log K_{eq} = 7.73 \tag{4}$$

$$Hfo\_wOH + SeO_4^{-2} = Hfo\_wOHSeO_4^{-2} \quad \log K_{eq} = 0.8 \tag{5}$$

$$Hfo\_wOH + UO_2(CO_3)_2^{2-} = Hfo\_wOUO_2(CO_3)_2^{3-} + H^+ \quad \log K_{eq} = -1.66 \tag{6}$$

$$H^+ + Hfo\_wOH + UO_2(CO_3)_3^{4-} = Hfo\_wOH_2UO_2(CO_3)_3^{3-} \quad \log K_{eq} = 13.71 \tag{7}$$

$$2Hfo\_wOH + HVO_4^{2-} = Hfo\_w_2O_2VO(OH) + 2OH^- \quad \log K_{eq} = 0.01 \tag{8}$$

$$2Hfo\_wOH + H_2VO_4^- = Hfo\_w_2O_2V(OH)_2^+ + 2OH^- \quad \log K_{eq} = -6.48 \tag{9}$$

$$Hfo\_wOH + Mn^{2+} = Hfo\_wOMn^+ + H^+ \quad \log K_{eq} = -3.5. \tag{10}$$

PHREEQC simulations showed decreasing sorption for all four anions Sb, Se, U, and V with increasing pH (Fig. 7). For example, Sb, Se, U and V were 93%, 99%, 56%, and 99% sorbed, respectively, at pH 8.2 (pe 4); whereas, these elements were 27%, 0%, 43%, and 10% sorbed at pH 9.2 (pe 7). The simulations also showed that aqueous concentrations of Sb, Se, U, and V increased proportionately to decreasing sorbed concentrations (Fig. 7).

The dominant surface species for Se was $Hfo\_wOHSeO_3^{2-}$ (Eq. (3)), as selenite ($HSeO_3^-$) species showed a stronger tendency to sorb than selenate (SeO_4^{2-}) species. The dominant surface species for U and V were $Hfo\_wOUO_2(CO_3)_2^{3-}$ (Eq. 6) and $Hfo\_w_2O_2VO(OH)$ (Eq. 8), respectively.

The PHREEQC simulations (Fig. 7) are consistent with the hypothesis that Sb, Se, U, and V removal from the water column during nighttime hours occur via sorption to metal oxide-coated

stationary surfaces, e.g. sediment or submerged aquatic vegetation. During daytime hours, Sb, Se, U, and V may be introduced to the water column via desorption from these phases. These trends are also consistent with experimental results that show decreased sorption with increasing pH (considering aqueous species discussed above) for Sb (Leuz et al., 2006; Tighe et al., 2005), Se (Duc et al., 2006; Hyun et al., 2006; Martínez et al., 2006), U (at alkaline pH; Farrell et al., 1999; Wazne et al., 2003), and V (Naeem et al., 2007).

In contrast to the anions (Sb, Se, U, and V), PHREEQC simulations showed the opposite trend for sorption of the cation Mn, with a slight increase from 45% to 54% in sorbed Mn concomitant with increased pH from 8.2 to 9.2 (Fig. 7). The observed trends are consistent with pH-driven sorption/desorption of Mn, but PHREEQC simulations also predict pH- and oxidation-driven precipitation of Mn minerals above pH 8.9 (pe 6); hence, both processes may contribute to the observed diel cycle.

The presence of elevated concentrations of Sb, Se, U, V, and Mn on sediment (see Section 3.1) is consistent with sorption/desorption of these elements to/from the sediment. The sediment may behave as a reservoir that releases/sorbs Sb, Se, U, V, and Mn due to shifting pH throughout the diel cycle.

Although pH-driven sorption conceptually describes the observed diel trends in concentrations of Sb, Se, U, V, and Mn, temperature may also be an important driver of sorption. Enthalpies of adsorption were set to zero in the PHREEQC simulations described above (values were generally not available); whereas sorption of anions and cations onto hydrous metal oxides is exothermic and endothermic, respectively (Machesky, 1990; Nimick et al., 2003), causing anion sorption to be favored by decreased temperature, and cation sorption to be favored by increased temperature. The extent to which the temperature cycle contributes to the observed diel cycles was not examined here; however, sorption may be driven by a combination of pH and temperature change (Gammons et al., 2005, 2007; Nimick et al., 2003; Parker et al., 2007; Shope et al., 2006). Nimick et al. (2003), using the theoretical basis and enthalpy values from Machesky (1990), calculated a doubling in aqueous concentrations of divalent metals with a 10 °C decrease in temperature (similar to what was measured at ADC-1 and ADC-2 during August 2008) assuming an adsorption enthalpy of +50 kJ/mol (on the order of enthalpies for Mn adsorption onto hydrous metal oxide surfaces). Furthermore, assuming an adsorption enthalpy of −38 kJ/mol for the anions (Gammons et al., 2005; Machesky, 1990), aqueous concentrations would decrease by half with a 10 °C decrease in temperature. Temperature and pH may both contribute to the sorption of Sb, Se, U, V, and Mn; however, on the basis of laboratory experiments Jones et al. (2004) concluded that pH was the major cause of diel Zn and As cycles, and Nimick et al. (2003) concluded that temperature is likely less important than pH in controlling sorption and diel metal cycles.

4.2. Origin of particulate pulses

The periodic nature of the pulses in unfiltered concentrations of particle-associated elements, combined with relatively constant concentrations in the filtered fraction of the same elements (excepting Mn), indicates that the pulses of particle-associated elements are not directly derived from chemical precipitation or sorption, but rather are derived from outside the water column, e.g. by the resuspension of settled (or otherwise immobilized) particles. On the basis of stage measurements, flow through the wetland ponds was relatively constant throughout the diel sampling periods (Fig. 2); thus, the pulses were not likely caused by changes in flow. Furthermore, there is no apparent recognizable temporal pattern in the particle-associated elements, making difficult the determination of a specific mechanism to produce the pattern. For example, during the 2008 sampling, the weather was clear and calm with wind speeds <5 m/s throughout much of the experiment (supporting information, Fig. S4); whereas during the 2009 sampling, an evening thunderstorm, with rain and wind speeds up to 17 m/s (supporting information, Fig. S4) punctuated the otherwise calm conditions. Notably, the pulses were greater during the 2008 sampling (calm conditions), suggesting that external processes such as re-suspension via wind, or delivery via runoff did not yield the observed pulses. Other possible processes include episodic upstream loads from metropolitan activities (e.g. treatment plants, industrial effluents, etc.), density-driven turnover of the water column (although it is difficult to envision how this would lead to multiple nighttime pulses), or resuspension of particles by bioturbation (e.g. swimming and feeding activities of carp that populate these wetland ponds). Settling and resuspension of particles has been shown to play an important role in trace element loads to water bodies (Owens et al., 2009), but predicting or modeling the temporal variations is difficult because the process is stochastic.

4.3. Interpretation of methylmercury concentrations

Wetlands are known to efficiently produce MeHg (e.g. Marvin-DiPasquale et al., 2003). Naftz et al. (this issue) showed that MeHg

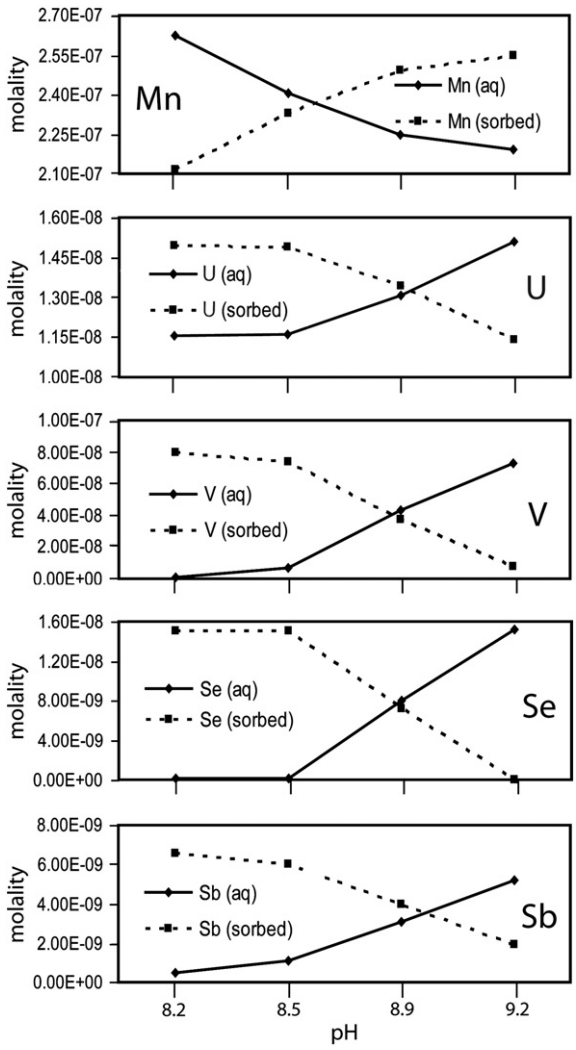

Fig. 7. Results of PHREEQC simulations of Mn, U, V, Se, and Sb sorption on hydrous ferric oxide (Hfo) from pH 8.2–9.2 showing modeled aqueous (solid line) and sorbed (dashed line) concentrations. Cation sorption (Mn) increased with increasing pH, and anion sorption (U, V, Se, and Sb) decreased with increasing pH.

production occurs during nighttime hours in a wetland located 30 km north of ADC. The MeHg production may have occurred in the oxygen-depleted water column (i.e. <1.0 mg/L DO), and possibly in the anoxic bottom waters with density-driven flux to the water column during nighttime hours. In pond ADC-2, increased MeHg was not detected (Fig. 6) during oxygen depletion of the water column (e.g., September 14–15, 2009, <0.5 mg/L DO; Fig. 2), indicating that MeHg production is spatially variable in the freshwater wetlands adjacent to GSL. Further examination of the processes governing Hg methylation in the GSL wetlands is needed.

4.4. Role of wetlands with respect to trace and major element loads to Great Salt Lake

Wetlands are generally perceived as important agents for improving water quality by reducing nutrient and trace element loads (e.g. Knowlton et al., 2002; Knox et al., 2006). Comparison of ADC-1 and ADC-2 clearly demonstrates attenuation of particle-associated trace elements between the two ponds, with concentration differences of particulate trace elements up to factors of 2–3 (Fig. 5). This attenuation occurs independent of the particulate pulses described above, and indicates that with respect to particulate elements ADC-2 is a net sink.

In contrast to particle-associated elements, dissolved elements showed relatively similar concentrations between the upstream and downstream ponds. Dissolved major ions Na^+, Cl^-, HCO_3^-, and SO_4^{2-} displayed slightly increased concentrations at ADC-2 relative to ADC-1, possibly due in part to evaporative concentration during transit (supporting information, Table S4). In contrast, NO_3^- was reduced by a factor of 3 from ADC-1 to ADC-2, indicating that the wetlands effectively remove NO_3^- through denitrification or uptake by biota. MeHg concentrations also decrease by a factor of 2 from ADC-1 to ADC-2 (Fig. 6), and factors governing this loss will be subject to further investigation.

For diel-cycling elements, subtracting elemental concentrations at ADC-1 from ADC-2 (inlet and outlet of ADC-2) shows production (positive values) or retention (negative values) within ADC-2, since there are no significant inflows between the two sites. For Sb, Se, V, and Mn, this difference varied on a diel cycle (Fig. 8; supporting information, Fig. S5). That this difference was time-varying indicates that retention/release of elements in the pond was also time-varying (were retention/release constant, the difference would have been constant). This demonstrates that the diel variation was driven *within* the pond, and was not inherited from upstream. For the anions, release was favored during daylight (high pH, lower sorption conditions) and retention was favored during nighttime (low pH, higher sorption conditions) (Fig. 8). The opposite was observed for the cation Mn (Fig. 8). Similar to the observed cycles in elemental concentrations, the cycling between retention and release is also consistent with pH-driven sorption/desorption. For V and Mn, the mean of the retention/release cycle was near zero, indicating no net retention or release over a 24-hr period. In contrast, the mean of the cycle for Sb was net positive, indicating Sb release from ADC-2 during the 24-hr period. The mean of the retention/release cycle for Se was negative, indicating net retention of Se in ADC-2 during the 24-hr period. Differences in net retention/release for Sb, Se, V, and Mn (Fig. 8) likely reflect the differences in the loads and retention capacities for these elements.

5. Conclusions

Previous observations of As diel cycling in aquatic systems have now been extended to include the trace element anions Sb, Se, U, and V. Similar to As, the diel cycles for Sb, Se, U, and V could be explained by pH-driven sorption/desorption to/from metal oxides in the stationary phase (e.g. sediment or submerged aquatic vegetation). In the case of Se, this pH-driven sorption/desorption was influenced by redox-driven transformation between selenate ($HSeO_3^-$, +IV oxidation state) and selenite (SeO_4^{2-}, +VI oxidation state) species.

Particle-associated elemental concentrations (e.g. Al, Fe, Pb, and Hg) showed much greater variations (i.e. up to a factor of 5) relative to the dissolved trace elemental concentrations during a 24-hr period. These pulses of particle-associated elements did not correlate to other measured parameters and were most likely due to stochastic processes such as bioturbation.

The lack of observed mercury methylation in these ponds under oxygen-depleted conditions, despite demonstrated mercury methylation in a nearby (<30 km) pond, demonstrates the high spatial variability of mercury methylation in the wetlands adjacent to Great Salt Lake.

With respect to the role of the wetland ponds in attenuating trace elements, retention of particle-associated elements was significant in ADC-2. Net retention occurred for some dissolved elements and net release occurred for other dissolved elements, likely reflecting differences in the loads and retention capacities for these elements.

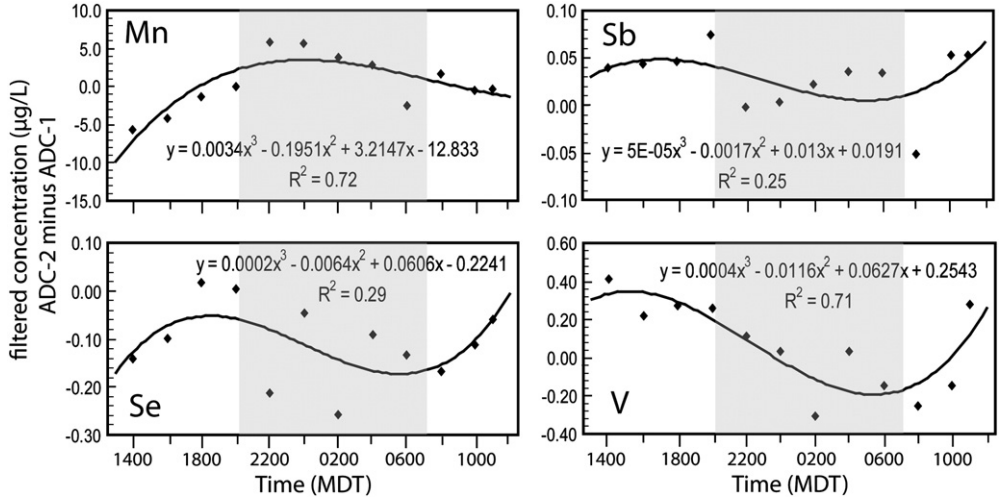

Fig. 8. Filtered concentration of diel-cycling elements Mn, Se, Sb, and V at ADC-2 minus ADC-1 from August 20–21, 2008 measurements. Shaded area indicates nighttime hours. Data trends were fitted with a third order polynomial as warranted by a substantial increase in R^2 relative to a linear trend line. Compare Fig. S5.

Acknowledgements

We would like to thank Dick Gilbert and Ambassador Duck Club for access to the sampling site, David Naftz for logistical help, equipment use, and discussions, David Tingey and Judy Steiger for help with analyzing samples, and Jay Cederberg, Kimberly Beisner, Wenjie Huang, Vishal Gupta, William Mace, and Danielle Fox for help with field work. This work was funded by the Division of Forestry Fire, and State Lands (FFSL) of the Utah Department of Natural Resources. We would like to thank the late Dave Grierson of FFSL for his support, and for making this study possible. We also wish to thank the two anonymous reviewers and guest editor Chris Gammons whose comments strengthened the manuscript and gave it more focused direction.

Appendix A. Supplementary data

Supplementary data to this article can be found online at doi:10.1016/j.chemgeo.2011.01.001.

References

Aldrich, T.W., Paul, D.S., 2002. Avian ecology of Great Salt Lake. In: Gwynn, J.W. (Ed.), Great Salt Lake: an Overview of Change. Utah Dept. of Natural Resources Special Publication, Salt Lake City, pp. 343–374.

Barringer, J.L., Wilson, T.P., Szabo, Z., Bonin, J.L., Fischer, J.M., Smith, N.P., 2008. Diurnal variations in, and influences on, concentrations of particulate and dissolved arsenic and metals in the mildly alkaline Wallkill River, New Jersey, USA. Environmental Geology 53 (6), 1183–1199.

Benoit, J.M., Gilmour, C.C., Heyes, A., Mason, R.P., Miller, C.L., 2003. Geochemical and biological controls over methylmercury production and degradation in aquatic ecosystems. In: Cai, Y., Braids, O.C. (Eds.), Biogeochemistry of Environmentally Important Trace Elements: Acs Symposium Series. Amer Chemical Soc, Washington, pp. 262–297.

Caudell, J.N., Conover, M.R., 2006. Energy content and digestibility of brine shrimp (*Artemia franciscana*) and other prey items of eared grebes (*Podiceps nigricollis*) on the Great Salt Lake, Utah. Biological Conservation 130 (2), 251–254.

Chavan, P.V., Dennett, K.E., Marchand, E.A., Gustin, M.S., 2007. Evaluation of small-scale constructed wetland for water quality and Hg transformation. Journal of Hazardous Materials 149 (3), 543–547.

Conover, M.R., Vest, J.L., 2009a. Selenium and mercury concentrations in California gulls breeding on the great Salt Lake, Utah, USA. Environmental Toxicology and Chemistry 28 (2), 324–329.

Conover, M.R., Vest, J.L., 2009b. Concentrations of selenium and mercury in eared grebes (*Podiceps nigricollis*) from Utah's Great Salt Lake, USA. Environmental Toxicology and Chemistry 28 (6), 1319–1323.

Deonarine, A., Hsu-Kim, H., 2009. Precipitation of mercuric sulfide nanoparticles in NOM-containing water: implications for the natural environment. Environmental Science and Technology 43 (7), 2368–2373.

Diaz, X., Johnson, W.P., Oliver, W.A., Naftz, D.L., 2009a. Volatile selenium flux from the Great Salt Lake, Utah. Environmental Science & Technology 43 (1), 53–59.

Diaz, X., Johnson, W.P., Fernandez, D., Naftz, D.L., 2009b. Size and elemental distributions of nano- to micro-particulates in the geochemically-stratified Great Salt Lake. Applied Geochemistry 24 (9), 1653–1665.

Dicataldo, G., Johnson, W.P., Naftz, D.L., Hayes, D.F., Moellmer, W.O., Miller, T., 2011. Diel variation of selenium and arsenic in a wetland of the Great Salt Lake, Utah. Applied Geochemistry 26 (1), 28–36.

Drott, A., Lambertsson, L., Bjorn, E., Skyllberg, U., 2007. Importance of dissolved neutral mercury sulfides for methyl mercury production in contaminated sediments. Environmental Science and Technology 41 (7), 2270–2276.

Duc, M., Lefèvre, G., Fédoroff, M., 2006. Sorption of selenite ions on hematite. Journal of Colloid and Interface Science 298 (2), 556–563.

Dzombak, D.A., Morel, F.M.M., 1990. Surface Complexation Modeling: Hydrous Ferric Oxide. Wiley, New York.

Farrell, J., Bostick, W.D., Jarabek, R.J., Fiedor, J.N., 1999. Uranium removal from ground water using zero valent iron media. Ground Water 37 (4), 618–624.

Filella, M., May, P.M., 2003. Computer simulation of the low-molecular-weight inorganic species distribution of antimony(III) and antimony(V) in natural waters. Geochimica et Cosmochimica Acta 67 (21), 4013–4031.

Fuller, C.C., Davis, J.A., 1989. Influence of coupling of sorption and photosynthetic processes on trace element cycles in natural waters. Nature 340 (6228), 52–54.

Gammons, C.H., Nimick, D.A., Parker, S.R., Cleasby, T.E., McCleskey, R.B., 2005. Diel behavior of iron and other heavy metals in a mountain stream with acidic to neutral pH: Fisher Creek, Montana, USA. Geochimica et Cosmochimica Acta 69 (10), 2505–2516.

Gammons, C.H., Grant, T.M., Nimick, D.A., Parker, S.R., DeGrandpre, M.D., 2007. Diel changes in water chemistry in an arsenic-rich stream and treatment-pond system. Science of the Total Environment 384, 433–451.

Gray, J.E., Hines, M.E., 2009. Biogeochemical mercury methylation influenced by reservoir eutrophication, Salmon Falls Creek Reservoir, Idaho, USA. Chemical Geology 258 (3–4), 157–167.

Hall, B.D., Aiken, G.R., Krabbenhoft, D.P., Marvin-DiPasquale, M., Swarzenski, C.M., 2008. Wetlands as principal zones of methylmercury production in southern Louisiana and the Gulf of Mexico region. Environmental Pollution 154 (1), 124–134.

Hyun, S., Burns, P.E., Murarka, I., Lee, L.S., 2006. Selenium(IV) and (VI) sorption by soils surrounding fly ash management facilities. Vadose Zone Journal 5 (4), 1110–1118.

Jones, C.A., Nimick, D.A., McCleskey, R.B., 2004. Relative effect of temperature and pH on diel cycling of dissolved trace elements in Prickly Pear Creek, Montana. Water Air and Soil Pollution 153 (1–4), 95–113.

Jung, J., Hyun, S.P., Lee, J.K., Cho, Y.H., Hahn, P.S., 1999. Adsorption of UO22+ on natural composite materials. Journal of Radioanalytical and Nuclear Chemistry 242 (2), 405–412.

Kerin, E.J., Gilmour, C.C., Roden, E., Suzuki, M.T., Coates, J.D., Mason, R.P., 2006. Mercury methylation by dissimilatory iron-reducing bacteria. Applied and Environmental Microbiology 72 (12), 7919–7921.

Knowlton, M.F., Cuvellier, C., Jones, J.R., 2002. Initial performance of a high capacity surface-flow treatment wetland. Wetlands 22 (3), 522–527.

Knox, A.S., Paller, M.H., Nelson, E.A., Specht, W.L., Halverson, N.V., Gladden, J.B., 2006. Metal distribution and stability in constructed wetland sediment. Journal of Environmental Quality 35 (5), 1948–1959.

Krabbenhoft, D.P., Hurley, J.P., Olson, M.L., Cleckner, L.B., 1998. Diel variability of mercury phase and species distributions in the Florida Everglades. Biogeochemistry 40 (2/3), 311–325.

Lambertsson, L., Nilsson, M., 2006. Organic material: the primary control on mercury methylation and ambient methyl mercury concentrations in estuarine sediments. Environmental Science & Technology 40 (6), 1822–1829.

Leuz, A.K., Monch, H., Johnson, C.A., 2006. Sorption of Sb(III) and Sb(V) to goethite: influence on Sb(III) oxidation and mobilization. Environmental Science & Technology 40 (23), 7277–7282.

Machesky, M.L., 1990. Influence of temperature on ion adsorption by hydrous metal oxides. Chemical Modeling of Aqueous Systems II. : In: Bassett, R.L., Melchoir, D.C. (Eds.), Am. Chem. Symp. Ser., V. 416. Am. Chem. Soc, Washington, D.C, pp. 282–292.

Mahoney, J.J., Cadle, S.A., Jakubowski, R.T., 2009. Uranyl adsorption onto hydrous ferric oxide—a re-evaluation for the diffuse layer model database. Environmental Science & Technology 43 (24), 9260–9266.

Martínez, M., Giménez, J., de Pablo, J., Rovira, M., Duro, L., 2006. Sorption of selenium (IV) and selenium(VI) onto magnetite. Applied Surface Science 252 (10), 3767–3773.

Martinez-Llado, X., de Pablo, J., Gimenez, J., Ayora, C., Marti, V., Rovira, M., 2008. Sorption of antimony (V) onto synthetic goethite in carbonate medium. Solvent Extraction and Ion Exchange 26 (3), 289–300.

Marvin-DiPasquale, M.C., Agee, J.L., Bouse, R.M., Jaffe, B.E., 2003. Microbial cycling of mercury in contaminated pelagic and wetland sediments of San Pablo Bay, California. Environmental Geology 43 (3), 260–267.

Marvin-Dipasquale, M.C., Lutz, M.A., Brigham, M.E., Krabbenhoft, D.P., Aiken, G.R., Orem, W.H., Hall, B.D., 2009. Mercury cycling in stream ecosystems. 2. Benthic methylmercury production and bed sediment-pore water partitioning. Environmental Science & Technology 43 (8), 2726–2732.

Mattuck, R., Nikolaidis, N.P., 1996. Chromium mobility in freshwater wetlands. Journal of Contaminant Hydrology 23 (3), 213–232.

McKnight, D., Bencala, K.E., 1988. Diel variations in iron chemistry in an acidic stream in the Colorado Rocky Mountains, USA. Arctic and Alpine Research 20 (4), 492–500.

Morel, F.M.M., Kraepiel, A.M.L., Amyot, M., 1998. The chemical cycle and bioaccumulation of mercury. Annual Review of Ecology and Systematics 29, 543–566.

Naeem, A., Westerhoff, P., Mustafa, S., 2007. Vanadium removal by metal (hydr)oxide adsorbents. Water Research 41 (7), 1596–1602.

Naftz, D., Angeroth, C., Kenney, T., Waddell, B., Darnall, N., Silva, S., Perschon, C., Whitehead, J., 2008. Anthropogenic influences on the input and biogeochemical cycling of nutrients and mercury in Great Salt Lake, Utah, USA. Applied Geochemistry 23 (6), 1731–1744.

Naftz, D.L., Cederberg, J.R., Krabbenhoft, D.P., Beisner, K.R., Whitehead, J., and Gardberg, J., this issue. Diurnal trends in methylmercury concentration in a wetland adjacent to Great Salt Lake, Utah, USA.

Nimick, D.A., Moore, J.N., Dalby, C.E., Savka, M.W., 1998. The fate of geothermal arsenic in the Madison and Missouri Rivers, Montana and Wyoming. Water Resources Research 34 (11), 3051–3067.

Nimick, D.A., Gammons, C.H., Cleasby, T.E., Madison, J.P., Skaar, D., Brick, C.M., 2003. Diel cycles in dissolved metal concentrations in streams: occurrence and possible causes. Water Resources Research 39 (9).

Nimick, D.A., Cleasby, T.E., McCleskey, R.B., 2005. Seasonality of diel cycles of dissolved metal concentrations in a Rocky Mountain stream. Environmental Geology 47 (5), 603–614.

Nimick, D.A., McCleskey, B.R., Gammons, C.H., Cleasby, T.E., Parker, S.R., 2007. Diel mercury-concentration variations in streams affected by mining and geothermal discharge. Science of the Total Environment 373 (1), 344–355.

Owens, E.M., Bookman, R., Effler, S.W., Driscoll, C.T., Matthews, D.A., Effler, A.J.P., 2009. Resuspension of mercury-contaminated sediments from an in-lake industrial waste deposit. Journal of Environmental Engineering 135 (7), 526–534.

Parker, S.R., Gammons, C.H., Jones, C.A., Nimick, D.A., 2007. Role of hydrous iron oxide formation in attenuation and diel cycling of dissolved trace metals in a stream affected by acid rock drainage. Water Air and Soil Pollution 181 (1–4), 247–263.

Parkhurst, D.L., Appelo, C.A.J., 1999. User's guide to PHREEQC (Version 2)—a computer program for speciation, batch-reaction, one-dimensional transport, and inverse geochemical calculations: US Geological Survey, Water-Resources Investigation Report 99-4259.

Peacock, C.L., Sherman, D.M., 2004. Vanadium(V) adsorption onto goethite (alpha-FeOOH) at pH 1.5 to 12: a surface complexation model based on ab initio molecular

geometries and EXAFS spectroscopy. Geochimica et Cosmochimica Acta 68 (8), 1723–1733.
Scholl, D.J., Ball, R.W., 2006. An evaluation of mercury concentrations in ducks from the Great Salt Lake, Utah for 2005 and 2006. Health Advisory Report. Utah Dept. of Health, Office of Epidemiology, Salt Lake City, UT, USA. 39 pp.
Shope, C.L., Xie, Y., Gammons, C.H., 2006. The influence of hydrous Mn–Zn oxides on diel cycling of Zn in an alkaline stream draining abandoned mine lands. Applied Geochemistry 21 (3), 476–491.
Sullivan, A.B., Drever, J.I., McKnight, D.M., 1998. Diel variation in element concentrations, Peru Creek, Summit County, Colorado. Journal of Geochemical Exploration 64 (1–3), 141–145.
Tarras-Wahlberg, N.H., Lane, S.N., 2003. Suspended sediment yield and metal contamination in a river catchment affected by El Nino events and gold mining activities: the Puyango river basin, southern Ecuador. Hydrological Processes 17 (15), 3101–3123.
Tighe, M., Lockwood, P., Wilson, S., 2005. Adsorption of antimony(v) by floodplain soils, amorphous iron(III) hydroxide and humic acid. Journal of Environmental Monitoring 7 (12), 1177–1185.
USEPA, 1982. Handbook for Sampling and Sample Preservation of Water and Wastewater. USEPA report EPA-600/4-82-029.
USEPA, 2000. Guidance for assessing chemical contaminant data for use in fish advisories, vol. 1, 3rd ed. : Fish Sampling and Analysis. USEPA Report EPA 823-B-00-007.
USEPA Method 1630, 2001. Methylmercury in Water by Distillation, Aqueous Ethylation, Purge and Trap, and CVAFS. January, 49 pp.
USEPA Method 1631, 2002. Revision E: Mercury in Water by Oxidation, Purge and Trap, and Cold Vapor Atomic Fluorescence Spectrometry. August, 38 pp.
USEPA Method 1669, 1996. Sampling Ambient Water for Trace Metals at EPA Water Quality Criteria Levels. July, 33 pp.
USEPA Method 1684, 2001. Total, Fixed, and Volatile Solids in Water, Solids, and Biosolids. Januray, 16 pp.
USEPA Method 354.1, 1983. Methods for Chemical Analysis of Water and Wastes.
USEPA Method 376.2, 1983. Methods for Chemical Analysis of Water and Wastes.
Vest, J.L., Conover, M.R., Perschon, C., Luft, J., Hall, J.O., 2009. Trace element concentrations in wintering waterfowl from the Great Salt Lake, Utah. Archives of Environmental Contamination and Toxicology 56 (2), 302–316.
Wazne, M., Korfiatis, G.P., Meng, X.G., 2003. Carbonate effects on hexavalent uranium adsorption by iron oxyhydroxide. Environmental Science & Technology 37 (16), 3619–3624.